

EXACT SOLUTION OF MULTI-LAYERED PIEZOELECTRIC CIRCULAR DIAPHRAGM WITH LINEAR SPRING AND SCREW SPRING

Lin-Quan Yao*

ABSTRACT

This paper investigates dynamic behavior of multi-layered piezoelectric circular diaphragms which are simplified as laminated circular plates with linear spring and screw spring. The simplified elastic support multi-layered plate model was adopted as simplified model. Using the classical laminated plate theory, mechanical, electrical and electromechanical characteristics of the multi-layered piezoelectric diaphragms have been studied. For ease of calculation, the dimensionless method was adopted. Furthermore, exact solution of this problem was carried out. Influence of dimensions of the laminar diaphragm and elastic coefficients on nature frequencies has also been studied. The thickness ratio of the PZT layer to the total thickness of the laminar diaphragm has been optimized to obtain the largest deflection.

Keywords: Piezoelectric, multi-layered circular plate, frequency

1. INTRODUCTION

Due to the intrinsic electromechanical coupling behaviors, piezoelectric materials have been widely used in fabrications of actuators and sensors, and MEMS [1]-[3]. Actuators or sensors in general are mainly made of multi-layered diaphragms (or films) with piezoelectric layers embedded (Figure 1). The multi-layered PZT diaphragms are not only used as a mechanic-electrical converter converting mechanical quantities (deformation, stress, velocity, acceleration, etc.) into suitable electrical signals but also be used as actuators converting electrical energies into mechanical ones. Therefore, the multi-layered PZT diaphragms are widely employed in MEMS devices.

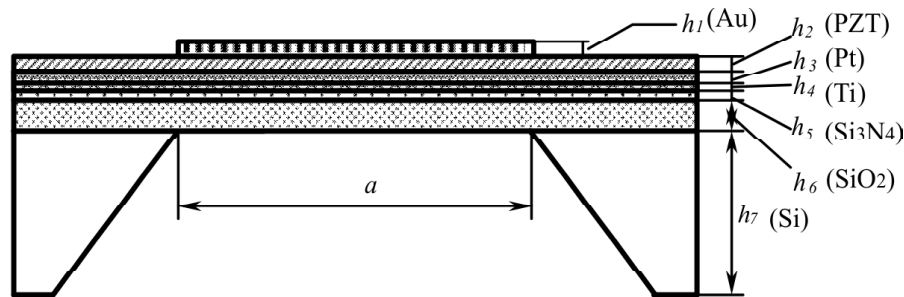


Figure 1: Sketch of Cross Section Model of Multi-layered Piezoelectric Diaphragm

Since the multi-layered PZT diaphragms play important roles in MEMS devices, many models have been proposed to investigate dynamic behaviors of the laminated structures [4]-[14], in which the approximate theories [5]-[8] and computational models [9], [10] have widely been used to predict dynamic characteristic of diaphragms. There is an increase trend in developing exact, closed and other accurate analytic solutions in recent years. Both coupled [7], [15] and uncoupled [6], [16] solutions have therefore been proposed. For piezoelectric actuators,

* School of Urban Rail Transportation, Soochow University, Suzhou, Jiangsu, 215006, P. R. China, E-mail: lqyao@suda.edu.cn

bending of rectangular plate [17]-[19], shell [20], multi-layered shell [21], circular plates [12]-[14], [22], and disk [23], [24] structures were induced by in-plane strains. Although some models have been developed to simulate symmetric [13] and asymmetric [15] rectangular piezoelectric/elastic plates, these models cannot be applied to multi-layered piezoelectric plates.

In most models, actuators or sensors were in general simplified into laminated plates with clamped supported boundary condition since the small ratio of the thickness of the multi-layered piezoelectric diaphragm to its other dimensions. However, the validity of such simplification has not been confirmed. In [25], the validity of the simplified clamped laminated plate models in the calculation of nature frequency is verified by comparison with the exact model. The frequency characteristics of the clamped rectangular multi-layered piezoelectric plates are then analytically investigated. However, there has the small error between exact model and simplified model. The elastic support boundary condition should be introduced for more close to exact model. This paper investigates dynamic behavior of multi-layered piezoelectric circular diaphragms which are simplified as elastic support laminated circular plates with spring. Using the classical laminated plate theory, mechanical, electrical and electromechanical characteristics of the multi-layered piezoelectric diaphragms have been studied. For ease of calculation, the dimensionless method was adopted. Furthermore, exact solution of this problem was carried out. Influence of dimensions of the laminar diaphragm and elastic coefficients on nature frequencies has also been studied. The thickness ratio of the PZT layer to the total thickness of the laminar diaphragm has been optimized to obtain the largest deflection.

2. THE SIMPLIFIED MODEL

The cross section configuration of the micro-piezoelectric thin film diaphragm is shown in Figure 1. The PZT film was deposited on Pt/Ti/Si₃N₄/SiO₂/Si wafer. Au layer was evaporated on the surface of PZT film as the top electrode. The backside silicon was wet-etched off till the SiO₂ layer. In figure 1, a is the diameter of circular laminated diaphragm, h_i ($i = 1\sim 6$) is the thickness of each film and they are 0.2mm, 0.6mm, 0.1mm, 0.05mm, 0.2mm and 0.5mm, respectively. h_7 is thickness of the substrate. The substrate is made of etched Si(100) wafer, the etched angle is known of around 54.7°.

In the clamped plate model, the boundary condition is considered to be rigid, even though the substrate and the deposited films are actually elastic. Therefore, there still exists small error in the frequencies between the exact model and the clamped plate model even the thickness of the substrate is very small or completely neglected. A relaxation in the clamped boundary on the clamped plate should be introduced [25]. Therefore, the laminated diaphragm shown in Figure 1 can be simplified as a disk of diameter a and the edge of the disk is elastic support with linear spring and screw spring as shown in Figure 2, in which k_1 and k_2 are elastic coefficients of linear spring and screw spring respectively. The constrain frame surrounding laminate can be taken off. An electrical field is applied on the upper (Au) and bottom (Pt) electrodes of the PZT (PbZr_{0.54}Ti_{0.46}O₃) film. The materials properties of each layer of the diaphragm are listed in Table 1.

Table 1
Material Properties

Material	E_p , GPa	ν_{12}	ρ , 10 ³ kg/m ³	e_{3p} C/m ²	κ_{33}^S , F/m	h_i , mm
Au	80	0.42	19.32			0.2
PbZr _{0.54} Ti _{0.46} O ₃	86.2	0.287	7.62	-7.279	3.106e-9	0.6
Pt	146.9	0.39	21.45			0.1
Ti	102.1	0.3	4.85			0.05
Si ₃ N ₄	150	0.24	3.24			0.2
SiO ₂	72.4	0.16	2.07			0.5
Si	70	0.35	2.699			

3. EQUATIONS OF MOTION

A multi-layered circular piezoelectric plate with elastic edges is adapted to study motion of the plate. Figure 3 shows the non-symmetric circular laminated plate with a diameter a that consists of n layers of films. The thickness

of the i th layer is h_i ($i = 1, \dots, n$), and the thickness of the piezoelectric layer is h_p ($1 \leq p \leq n$). In figure 3, h_0 is a distance from the top of the plate to X axes. Z_{i-1} and Z_i are the Z coordinate values at the top and the bottom surfaces of the i th layer. Thus, the following relation can be obtained:

$$Z_0 = h_0, Z_i = h_0 - \sum_{k=1}^i h_k, i = 1, 2, \dots, n, \quad (1)$$

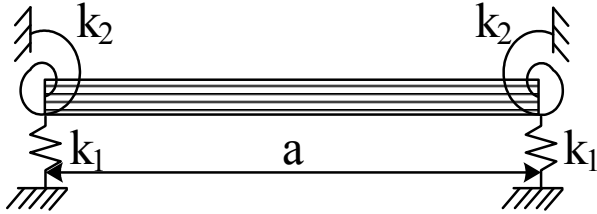


Figure 2: Simplified Model of Multi-layered Piezoelectric Diaphragm with Linear Spring and Screw Spring

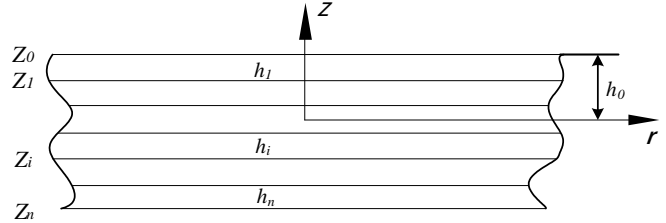


Figure 3: Side View of the Laminated Plate

(A) Displacement and Strain

For a circular plate with axisymmetric oscillations, the linear strains associated with the displacement can be expressed as

$$\begin{Bmatrix} \varepsilon_r \\ \varepsilon_\theta \\ \gamma_{r\theta} \end{Bmatrix} = \begin{Bmatrix} \varepsilon_r^0 \\ \varepsilon_\theta^0 \\ \gamma_{r\theta}^0 \end{Bmatrix} + z \begin{Bmatrix} \varepsilon_r^1 \\ \varepsilon_\theta^1 \\ \gamma_{r\theta}^1 \end{Bmatrix} = \begin{Bmatrix} \frac{\partial u_r}{\partial r} \\ \frac{u_\theta}{r} \\ \frac{\partial u_\theta}{\partial r} - \frac{u_\theta}{r} \end{Bmatrix} + z \begin{Bmatrix} -\frac{\partial^2 w}{\partial r^2} \\ -\frac{\partial w}{r \partial r} \\ 0 \end{Bmatrix}, \quad (2)$$

where (u_r, u_θ, w) are, respectively, the radial, circumferential and transverse displacements of a point on the plate at $z = 0$, $(\varepsilon_r, \varepsilon_\theta, \gamma_{r\theta})$ is the strain components, $(\varepsilon_r^0, \varepsilon_\theta^0, \gamma_{r\theta}^0) = \varepsilon^0$ is the membrane strains, and $(\varepsilon_r^1, \varepsilon_\theta^1, \gamma_{r\theta}^1) = \varepsilon^1$ is the flexural (bending) strains.

(B) Equilibrium Equation

Since only small strains, displacements and rotations are considered, the effect of the rotary inertia can be neglected. The transverse governing equations of the CLPT can be derived using the dynamic version of the principle of virtual displacement [26]:

$$\frac{\partial^2 M_r}{\partial r^2} + \frac{1}{r} \frac{\partial (2M_r - M_\theta)}{\partial r} + q = I_0 \ddot{w}, \quad (3)$$

where q is the distributed force at surface of the plate, and moment resultants and the mass moments of inertias are defined as

$$\mathbf{M} = \begin{Bmatrix} M_r \\ M_\theta \\ M_{r\theta} \end{Bmatrix} = \int_{z_n}^{z_0} \begin{Bmatrix} \sigma_r \\ \sigma_\theta \\ \tau_{r\theta} \end{Bmatrix} z dz, \quad I_0 = \int_{z_n}^{z_0} \rho_0 dz, \quad (4)$$

where $(\sigma_r, \sigma_\theta, \tau_{r\theta})$ are the radial, circumferential and shear stresses, respectively, and ρ_0 is the material density.

(C) Laminate Constitutive Equation

Assume that all deposited film and silicon substrate are transversely isotropic. The piezoelectric layer is polarized at the thickness direction, and its two surfaces are completely covered with electrodes. The linear constitutive relations for the piezoelectric lamina can be expressed by

$$\begin{Bmatrix} \sigma_r \\ \sigma_\theta \\ \tau_{r\theta} \end{Bmatrix} = \begin{bmatrix} C_{11} & C_{12} & 0 \\ C_{12} & C_{11} & 0 \\ 0 & 0 & C_{66} \end{bmatrix} \begin{Bmatrix} \varepsilon_r \\ \varepsilon_\theta \\ \gamma_{r\theta} \end{Bmatrix} - \begin{Bmatrix} e_{31} \\ e_{31} \\ 0 \end{Bmatrix} E_z \quad (1)$$

$$D_z = \begin{Bmatrix} e_{31} & e_{31} & 0 \end{Bmatrix} \begin{Bmatrix} \varepsilon_r \\ \varepsilon_\theta \\ \gamma_{r\theta} \end{Bmatrix} + \kappa_{33}^S E_z \quad (2)$$

where E_z and D_z are, respectively, electric field and electric displacement at Z direction; e_{31} and κ_{33}^S are, respectively, the plane-reduced piezoelectric constant and dielectric permittivities at a constant strains, that is, $e_{31} = e_{31}^E - e_{33}^E C_{13}^E / C_{33}^E$, $\kappa_{33}^S = \kappa_{33}^E + (e_{33}^E)^2 / C_{33}^E$, in which the superscript E mean that they are three-dimensional piezoelectric, dielectric and elastic constants. The plane stress-reduced stiffness coefficients C_{11} , C_{12} , C_{66} are known in terms of the engineering constants (E , ν):

$$C_{11} = \frac{E}{1-\nu^2}, \quad C_{12} = \frac{\nu E}{1-\nu^2}, \quad C_{66} = \frac{E}{2(1+\nu)} = \frac{C_{11} - C_{12}}{2}. \quad (3)$$

Note that the piezoelectric coefficients are zero for non-piezoelectric layer in and .

(D) Simplified Equation of Motion

The electric potential is assumed to quadratic function with regard to z :

$$\phi = \phi_0 + z\phi_1 + z^2\phi_2. \quad (4)$$

The electrical displacement D_z is constant with respect to the plate thickness as

$$D_z = D_3^0. \quad (5)$$

The electrical boundary conditions for the piezoelectric layer with fully covered electrodes are:

$$\phi|_{z=z_{p-1}} = V_1 \text{ and } \phi|_{z=z_p} = V_2. \quad (6)$$

Substituting (6) into (4), it yields

$$\phi_1 = \frac{V_1 - V_2}{h_p} - 2z_c^p \phi_2 \quad (7)$$

where z_c^p is the distance from the $Z = 0$ coordinate plane to the mid-plane of piezoelectric layer, that is, $z_c^p = (z_{p-1} + z_p) / 2$.

According to (4), the electric field can be expressed as

$$E_z = -\frac{\partial \phi}{\partial z} = -\phi_1 - 2z\phi_2 = E_z^0 + zE_z^1. \quad (8)$$

Substituting (5) and (8) into (2) through (7), it yields

$$E_z^0 = \frac{V_2 - V_1}{h_p} + \frac{e_{31} z_c^p}{\kappa_{33}^S} (\varepsilon_r^1 + \varepsilon_\theta^1), \quad E_z^1 = -\frac{e_{31}}{\kappa_{33}^S} (\varepsilon_r^1 + \varepsilon_\theta^1). \quad (9)$$

Substituting (8) through (9) into (1), the membrane stresses, $(\sigma_r^0, \sigma_\theta^0, \sigma_{r\theta}^0)$ and flexural stresses, $(\sigma_r^1, \sigma_\theta^1, \sigma_{r\theta}^1)$ can respectively be obtained as

$$\begin{Bmatrix} \sigma_r^0 \\ \sigma_\theta^0 \\ \tau_{r\theta}^0 \end{Bmatrix} = \begin{bmatrix} C_{11} & C_{12} & 0 \\ C_{12} & C_{11} & 0 \\ 0 & 0 & C_{66} \end{bmatrix} \begin{Bmatrix} \varepsilon_r^0 \\ \varepsilon_\theta^0 \\ \gamma_{r\theta}^0 \end{Bmatrix} - C_p z_c^p \begin{bmatrix} 1 & 1 & 0 \\ 1 & 1 & 0 \\ 0 & 0 & 0 \end{bmatrix} \begin{Bmatrix} \varepsilon_r^1 \\ \varepsilon_\theta^1 \\ \gamma_{r\theta}^1 \end{Bmatrix} + \frac{e_{31}(V_1 - V_2)}{h_p} \begin{Bmatrix} 1 \\ 1 \\ 0 \end{Bmatrix} \quad (10)$$

$$\begin{Bmatrix} \sigma_r^1 \\ \sigma_\theta^1 \\ \tau_{r\theta}^1 \end{Bmatrix} = \begin{bmatrix} C_{11} + C_p & C_{12} + C_p & 0 \\ C_{12} + C_p & C_{11} + C_p & 0 \\ 0 & 0 & C_{66} \end{bmatrix} \begin{Bmatrix} \varepsilon_r^1 \\ \varepsilon_\theta^1 \\ \gamma_{r\theta}^1 \end{Bmatrix} \quad (11)$$

where $C_p = e_{31}^2 / \kappa_{33}^S$.

Substituting (1) into using (10) and (11), the membrane forces and bending moments can be obtained as

$$\mathbf{M} = \mathbf{B}\boldsymbol{\varepsilon}^0 + \mathbf{D}\boldsymbol{\varepsilon}^1 - \mathbf{M}^p \quad (12)$$

where

$$\mathbf{M} = \begin{Bmatrix} M_r \\ M_\theta \\ M_{r\theta} \end{Bmatrix}, \quad \mathbf{M}^p = \begin{Bmatrix} M_r^p \\ M_\theta^p \\ M_{r\theta}^p \end{Bmatrix} = \begin{Bmatrix} e_{31} z_c^p (V_2 - V_1) \\ e_{31} z_c^p (V_2 - V_1) \\ 0 \end{Bmatrix}, \quad (13)$$

$$\mathbf{B} = \begin{bmatrix} B_{11} & B_{12} & 0 \\ B_{12} & B_{11} & 0 \\ 0 & 0 & B_{66} \end{bmatrix}, \quad \mathbf{D} = \begin{bmatrix} D_{11} & D_{12} & 0 \\ D_{12} & D_{11} & 0 \\ 0 & 0 & D_{66} \end{bmatrix}, \quad (14)$$

$$B_m = \frac{1}{2} \sum_{k=1}^n C_m^{(k)} h_k (z_{k-1} + z_k), \quad D_m = \frac{1}{3} \sum_{k=1}^n C_m^{(k)} (z_{k-1}^3 - z_k^3) + \frac{C_p h_p^3}{12} \delta_0, \quad (15)$$

in which $m = 11, 12, 66$, and $\delta_0 = 0$ for $m = 66$ and $\delta_0 = 1$ for $m = 11$ or 12 .

From (3), it is known:

$$B_{11} - B_{12} = 2B_{66}, \quad D_{11} - D_{12} = 2D_{66}. \quad (16)$$

To simplify controlling equations, the coordinate h_0 is redefined as the reference plane such that $B_{11} = 0$. From and (15), it can be deduced that:

$$h_0 = \frac{1}{2} \sum_{k=1}^n \left[C_{11}^{(k)} h_k \left(2 \sum_{i=1}^k h_i - h_k \right) \right] / \sum_{k=1}^n C_{11}^{(k)} h_k. \quad (17)$$

Substituting (12) into through and , and condition $B_{11} = 0$, the equations of motion in terms of displacements can be obtained as

$$-D_{11} \left(\frac{\partial^4}{\partial r^4} + \frac{2}{r} \frac{\partial^3}{\partial r^3} - \frac{1}{r^2} \frac{\partial^2}{\partial r^2} + \frac{1}{r^3} \frac{\partial}{\partial r} \right) w(r, t) + q(r, t) = I_0 \ddot{w}(r, t) \quad (18)$$

Equation is the simplified motion equation in terms of displacement. According to , the in-plane membrane vibration is no longer coupled from the bending vibration. Hence, only the bending vibration equation under the boundary conditions is necessary to be considered.

For the elastic edge and center point, the displacement boundary conditions are

$$Q = -D_{11} \frac{\partial}{\partial r} \frac{1}{r} \frac{\partial}{\partial r} r \frac{\partial w}{\partial r} = k_1 w, \text{ at } r = a/2, \quad (19)$$

$$M_r = -D_{11} \left(\frac{\partial^2 w}{\partial r^2} + \frac{\bar{\nu}}{r} \frac{\partial w}{\partial r} \right) - M_r^p = k_2 \frac{\partial w}{\partial r}, \text{ at } r = a/2, \quad (20)$$

$$w < \infty, \quad \frac{\partial w}{\partial r} = 0, \text{ at } r = 0. \quad (21)$$

where, k_1, k_2 are elastic coefficients of linear spring and screw spring respectively, $\bar{\nu} = D_{12} / D_{11}$.

4. CALCULATION METHODOLOGY

If the structure subjects to the time harmonic loading at a circular frequency ω , the displacements and sensor voltage are also time harmonic with the same frequency. They can be expressed as

$$q(r, t) = \tilde{q}(r) e^{i\omega t}, \quad w(r, t) = W(r) e^{i\omega t}, \quad V_s = \tilde{V} e^{i\omega t}, \quad M_r^p = \tilde{M}^p e^{i\omega t} = e_{31} z_c^p (\tilde{V}_2 - \tilde{V}_1) e^{i\omega t}. \quad (22)$$

Substituting (22) into (18), the bending governing differential equations of mode shape $W(r)$ can be obtained:

$$D_{11} \left(\frac{d^4}{dr^4} + \frac{2}{r} \frac{d^3}{dr^3} - \frac{1}{r^2} \frac{d^2}{dr^2} + \frac{1}{r^3} \frac{d}{dr} \right) W(r) - \omega^2 I_0 W(r) = \tilde{q}(r). \quad (23)$$

Corresponding to (23), mechanical boundary conditions for the elastic edge (19) and center point (21) are

$$-D_{11} \frac{d}{dr} \frac{1}{r} \frac{d}{dr} r \frac{dW}{dr} = k_1 W, \text{ at } r = a/2, \quad (24)$$

$$-D_{11} \left(\frac{d^2 W}{dr^2} + \frac{\bar{\nu}}{r} \frac{dW}{dr} \right) - \tilde{M} = k_2 \frac{dW}{dr}, \text{ at } r = a/2, \quad (25)$$

$$W < \infty, \quad \frac{dW}{dr} = 0, \text{ at } r = 0. \quad (26)$$

Generally, because the dimension of the structure is very small, it may cause additional calculation error, even float data overflow. To avoid data flow and reduce the calculated error, following dimensionless parameters are therefore introduced:

$$\xi = \frac{2r}{a}, \quad \bar{\omega} = \gamma^2 = \frac{\omega a^2}{4} \sqrt{\frac{I_0}{D_{11}}}, \quad \bar{q} = \frac{\tilde{q} a^4}{16hD_{11}}, \quad \bar{M} = \frac{a^2}{4D_{11}h} \tilde{M}, \quad \bar{W}(r) = \frac{W(r)}{h}, \quad (27)$$

$$f = \frac{\omega}{2\pi} = \frac{2\bar{\omega}}{\pi a^2} \sqrt{\frac{D_{11}}{I_0}}, \quad K_1 = \frac{a^3 k_1}{8D_{11}}, \quad K_2 = \frac{ak_2}{2D_{11}} \quad (28)$$

where $\bar{\omega}$ and γ is the frequency parameter, f is nature frequency. The governing equation (23), and boundary conditions (24) ~ (26) can be expressed by dimensionless parameters:

$$\frac{d^4 \bar{W}}{d\xi^4} + \frac{2}{\xi} \frac{d^3 \bar{W}}{d\xi^3} - \frac{1}{\xi^2} \frac{d^2 \bar{W}}{d\xi^2} + \frac{1}{\xi^3} \frac{d\bar{W}}{d\xi} - \gamma^4 \bar{W} = \bar{q} \quad (29)$$

$$\frac{d}{d\xi} \frac{1}{\xi} \frac{d}{d\xi} \xi \frac{d\bar{W}}{d\xi} + K_1 \bar{W} = 0, \text{ at } \xi = 1 \quad (30)$$

$$\frac{d^2\bar{W}}{d\xi^2} + \left(K_2 + \frac{\bar{v}}{\xi} \right) \frac{d\bar{W}}{d\xi} + \bar{M} = 0, \text{ at } \xi = 1 \tag{31}$$

$$\bar{W} < \infty, \frac{d\bar{W}}{d\xi} = 0, \text{ at } \xi = 0 \tag{32}$$

Let load and electric potential be zero for free vibration. Then the complete solution of equation (29) is:

$$\bar{W} = C_1 J_0(\gamma\xi) + C_2 N_0(\gamma\xi) + C_3 I_0(\gamma\xi) + C_4 K_0(\gamma\xi) \tag{33}$$

where C_i ($i = 1 \sim 4$) are constants determined by boundary conditions (30) ~ (32), J_0, N_0, I_0, K_0 are, respectively, Bessel functions of the first kind of zero order, Bessel functions of the second kind of zero order, modified Bessel functions of the first kind of zero order and modified Bessel functions of the second kind of zero order. Since no external force acts at the center, the solution must be finite for $x = 0$, i.e. condition (32), thus, C_2 and C_4 must be zero. The solution will then be given by:

$$\bar{W} = C_1 J_0(\gamma\xi) + C_3 I_0(\gamma\xi) \tag{34}$$

According to boundary conditions (30) and (31), constants C_1 and C_3 should satisfy following equations.

$$\begin{cases} [\gamma^3 J_1(\gamma) + K_1 J_0(\gamma)]C_1 + [\gamma^3 I_1(\gamma) + K_1 I_0(\gamma)]C_3 = 0 \\ [-\gamma J_0(\gamma) + (K_2 + \bar{v} - 1)J_1(\gamma)]C_1 + [\gamma I_0(\gamma) + (K_2 + \bar{v} - 1)I_1(\gamma)]C_3 = 0 \end{cases} \tag{35}$$

where J_1 and I_1 are Bessel function of the first type of one order and modified Bessel function of the second kind of one order, respectively. In order to obtain nonzero solution in equation (35) with respect to C_1 and C_3 , its determinant made up of the coefficients is equal to zero, which results in the characteristic equation for determining the natural frequency parameter (γ) as

$$\begin{vmatrix} \gamma^3 J_1(\gamma) + K_1 J_0(\gamma) & \gamma^3 I_1(\gamma) + K_1 I_0(\gamma) \\ -\gamma J_0(\gamma) - (K_2 + \bar{v} - 1)J_1(\gamma) & \gamma I_0(\gamma) + (K_2 + \bar{v} - 1)I_1(\gamma) \end{vmatrix} = 0 \tag{36}$$

Equation (36) results in the n-th order characteristic equation for determining the natural frequencies. The exact

nature frequencies can be obtained by means of formulae $f = \frac{2\gamma^2}{\pi a^2} \sqrt{\frac{D_{11}}{I_0}}$ if only the parameters are calculated.

Especially, the frequency equations with regard to several ordinarily boundary conditions can be obtained from equation as follows:

- (a) The clamped boundary condition ($k_1 = \infty, k_2 = \infty$): $J_0(\gamma) I_1(\gamma) + J_1(\gamma) I_0(\gamma) = 0$.
- (b) The simply supported boundary condition ($k_1 = \infty, k_2 = 0$): $J_0(\gamma)(\gamma I_0(\gamma) + (\bar{v} - 1)I_1(\gamma)) + I_0(\gamma)(\gamma J_0(\gamma) + (\bar{v} - 1)J_1(\gamma)) = 0$.
- (c) The free boundary condition ($k_1 = 0, k_2 = 0$): $J_1(\gamma)(\gamma I_0(\gamma) + (\bar{v} - 1)I_1(\gamma)) + I_1(\gamma)(\gamma J_0(\gamma) + (\bar{v} - 1)J_1(\gamma)) = 0$.
- (d) The elastic embedding fixed boundary condition ($k_1 = \infty$): $J_1(\gamma)(\gamma I_0(\gamma) + (K_2 + \bar{v} - 1)I_1(\gamma)) + I_1(\gamma)(\gamma J_0(\gamma) + (K_2 + \bar{v} - 1)J_1(\gamma)) = 0$.
- (e) The elastic support boundary condition ($k_2 = \infty$): $I_1(\gamma) (\gamma^3 J_1(\gamma) + K_1 J_0(\gamma)) + J_1(\gamma) (\gamma^3 I_1(\gamma) + K_1 I_0(\gamma)) = 0$.

5. NUMERICAL ANALYSIS

(A) Frequency Parameters

First, the frequency parameters $\gamma = \sqrt{\omega}$ for several common boundary cases are calculated and listed in Table 2. Second, Table 3 lists the frequency parameter for various dimensionless elastic coefficients (K_1, K_2) for the first five

vibration modes. Lastly, in order to observe expressly the frequency parameters various with dimensionless elastic coefficients K_1 and K_2 , figures 4-6 show their relative change cures. In these figures, the relative change is defined as

$$\delta_i = (\gamma_i(K_1, K_2) - \gamma_i(K_1, 0)) / \gamma_i(K_1, 0), i = 1, 2, 3, 4, 5, \text{ for given } K_1$$

Because of the frequency parameters after first mode change very small, the only frequency parameter γ_1 is shown in figure 7. From Tables 3 or Figures 4 ~7, it can obtain the following conclusions: (1) When given coefficient K_2 , the frequency parameters are increased with elastic coefficient K_1 . The first frequency parameter is rapidly increased with the increase of elastic coefficient K_1 , especially $K_1 < 10$. However, it is slowly increased when $K_1 > 10$. (2) The first frequency parameter change is the largest among all, that is, $\delta_1 > \delta_2 > \delta_3 > \delta_4 > \delta_5$. (3) When given coefficient K_1 , the first frequency parameters are decreased with elastic coefficient K_2 . The larger the coefficient K_1 is, the less first frequency parameter decreases. (4) Frequency parameters, especially first frequency parameter depend on parameter $K_1 (< 10)$ (linear spring) markedly and depend on parameter K_2 (screw spring) slowly.

Table 2
Frequency Parameters γ for the First Five Modes at Several Common Boundary Cases

(K_1, K_2)	γ				
	γ_1	γ_2	γ_3	γ_4	γ_5
$K_1 = K_2 = \infty$ (clamped)	3.1962	6.3064	9.4395	12.5771	15.7164
$K_1 = \infty, K_2 = 0$ (simply supported)	2.2116	5.4485	8.6095	11.7595	14.9058
$K_1 = 0, K_2 = 0$ (free)	2.9895	6.1952	9.3642	12.5203	15.6708

Table 3
Frequency Parameters vs. various Elastic Coefficients (K_1, K_2) for the First Five Vibration Modes

K_1	K_2	γ_1	γ_2	γ_3	γ_4	γ_5
0.0	0.0	2.9895	6.1952	9.3642	12.5203	15.6708
	1.0	3.2488	6.3409	9.4643	12.5965	15.7322
	5.0	3.5686	6.6277	9.7070	12.8038	15.9122
	50	3.7950	6.9505	10.0818	13.2071	16.3306
	∞	3.8317	7.0156	10.1735	13.3237	16.4706
1.0	0.0	2.9477	6.1906	9.3630	12.5198	15.6705
	1.0	3.2207	6.3370	9.4632	12.5960	15.7320
	5.0	3.5526	6.6249	9.7061	12.8033	15.9120
	50	3.7853	6.9488	10.0812	13.2068	16.3305
	∞	3.8229	7.0141	10.1730	13.3235	16.4705
5.0	0.0	2.7875	6.1739	9.3581	12.5177	15.6695
	1.0	3.1110	6.3217	9.4585	12.5940	15.7310
	5.0	3.4899	6.6135	9.7022	12.8016	15.9110
	50	3.7474	6.9421	10.0789	13.2058	16.3299
	∞	3.7883	7.0084	10.1711	13.3226	16.4701
50	0.0	2.3079	6.0088	9.3055	12.4952	15.6579
	1.0	2.6124	6.1680	9.4080	12.5720	15.7196
	5.0	3.0728	6.4949	9.6599	12.7822	15.9006
	50	3.4527	6.8714	10.0537	13.1940	16.3234
	∞	3.5161	6.9470	10.1502	13.3132	16.4651
	0.0	2.2116	5.4485	8.6095	11.7595	14.9058
	1.0	2.4571	5.5439	8.6691	11.8029	14.9499
	5.0	2.8155	5.7837	8.8458	11.9421	15.0545
	50	3.1364	6.1952	9.2822	12.3789	15.4817
	∞	3.1962	6.3064	9.4395	12.5771	15.7164

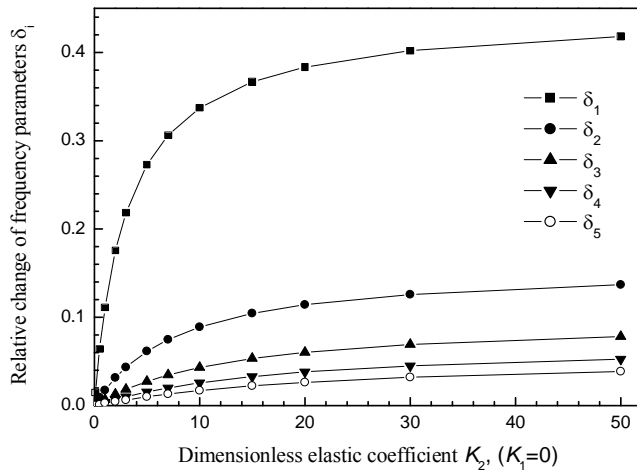


Figure 4: Relative Change of the First Five Frequency Parameters via Dimensionless Elastic Coefficient K_1 ($K_2 = 0$)

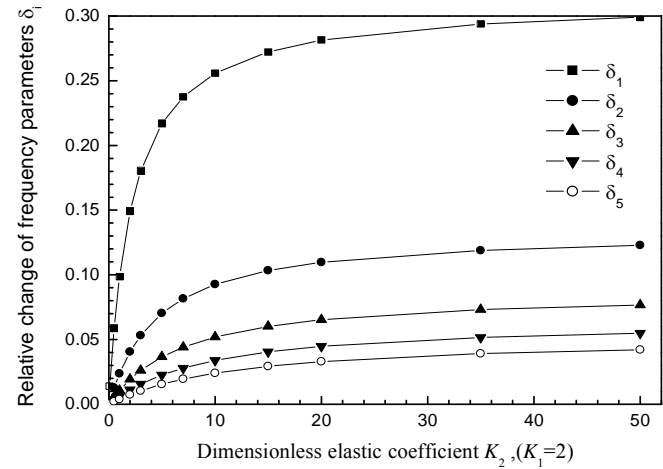


Figure 5: Relative Change of the First Five Frequency Parameters via Dimensionless Elastic Coefficient K_1 ($K_2 = 2$)

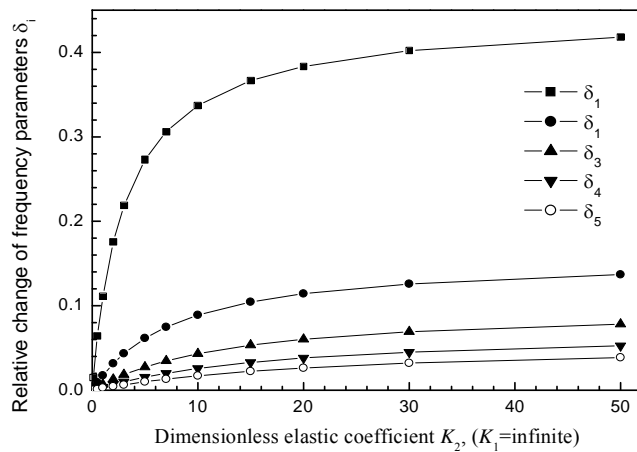


Figure 6: Relative Change of First Five Frequency Parameters via Dimensionless Elastic Coefficient K_1 ($K_2 = \infty$)

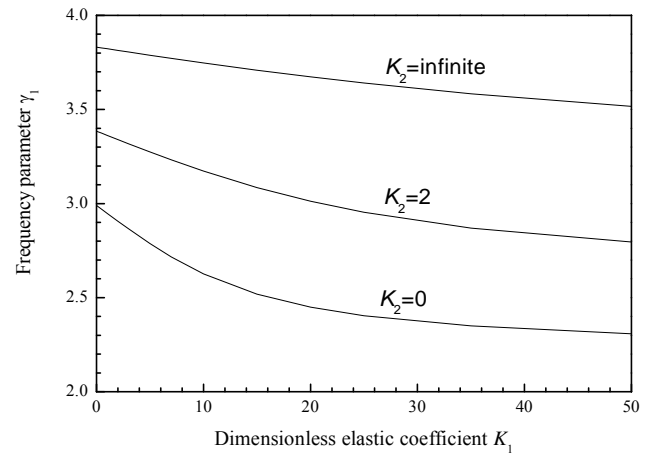


Figure 7: Change of the First Frequency Parameters (γ_1) via Dimensionless Elastic Coefficient (K_1)

(B) Dimension Effect of Diaphragm on Nature Frequency

In this part, clamped boundary condition is considered. The influence of the diameter of circular laminar diaphragm with different thicknesses of piezoelectric layer, $h_p = 0.6 \text{ mm}, 2.4\text{mm}, 4.2\text{mm}, 6.0\text{mm}$ on the first nature frequency is shown in figure 8. The frequency values decrease rapidly with the increase of the diameter, especially in the small diameter range. Through varying thickness of the PZT films and diameter of the clamped circular plate, the required resonance frequency can be obtained. For example, for the PZT films with thickness of 0.6mm , the resonance frequency of the diaphragm with diameter of $1000\mu\text{m}$ to $300\mu\text{m}$ are at the range of 10 kHz to 100 kHz . This frequencies range is particularly suitable for the ultrasonic audio applications. Because the first frequency is inverse proportion to square of diameter of the circular plate, a simple and easy used linear relation on frequencies could be obtained as we change x-coordinate in to the reciprocal of area of diaphragm, $4/(\pi a^2)$, shown in figure 9.

(C) Thickness Ratio Effect on the Nature Frequency

The nature frequency of the diaphragm varies with the thickness of the piezoelectric film. Figure 10 shows the influence of piezoelectric film thickness on the frequency factor f versus the thickness ratio a , where a is thickness ratio between the thickness of the PZT layer and the total thickness of plate. It is assumed that the total thickness is a constant while the thickness of the PZT film varies with the ratio a , other layer's thicknesses hold the line, namely,

$$h = 1.65 \mu\text{m}, h_p = \alpha h, h_m = h_1 + h_3 + h_4 + h_5 = 0.55 \mu\text{m}, h_6 = (1 - \alpha) h - h_m = 1.1 - 1.65\alpha (\mu\text{m})$$

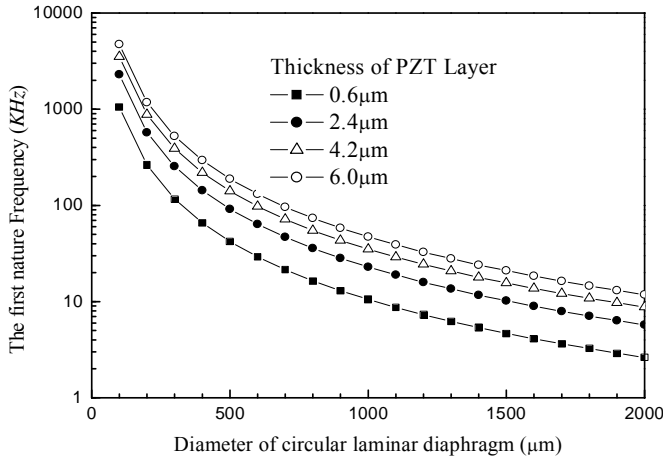


Figure 8: Change of the First Nature Frequency via the Variation of Diameter of Circular Diaphragm

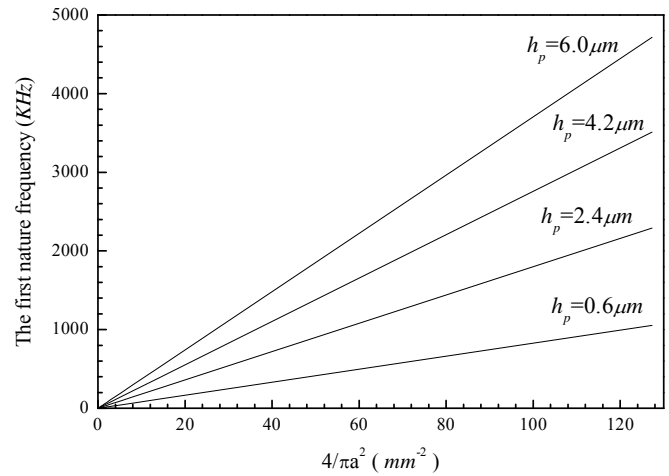


Figure 9: Change of the First Nature Frequency via the Variation of Inverse of Area ($4/\pi a^2$) of Circular Diaphragm

The range of a is therefore $0 < \alpha < 1 - \frac{h_m}{h} = \frac{2}{3}$. From figure 10, the optimized thickness ratio can be obtained to be 0.42 for $\text{PbZr}_{0.54}\text{Ti}_{0.46}\text{O}_3$, at which the largest deflection can be obtained. It is note that same optimized thickness ratio is obtained for other different diameter.

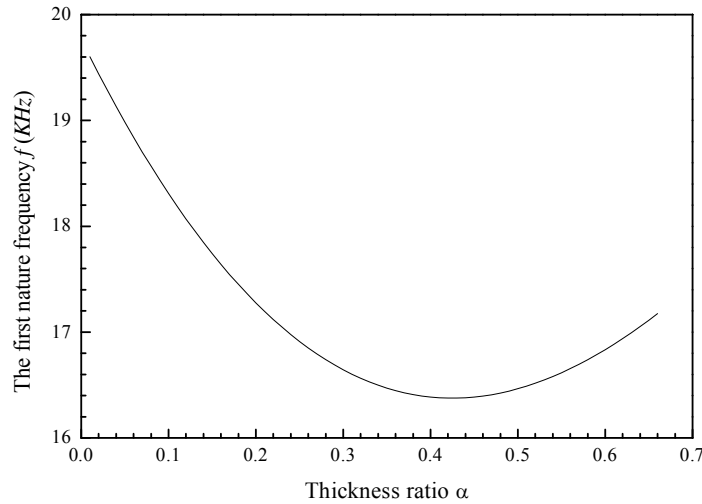


Figure 10: Dependence of the Thickness Ration of Piezoelectric Layer on the Frequency ($a = 800\mu\text{m}$)

6. CONCLUSIONS

The analytical model of the multi-layered laminated elastic support circular plates was formulated using the electro-elastic theory and classical laminated plate theory. The dimensionless governing differential equations were derived and solved. The exact solution of the laminated elastic support circular plate can be applied in many different cases, such as laminates containing any numbers of layer, and laminates with different thickness and diameter, etc.

The influence of elastic coefficients of the support condition of laminar diaphragm on the nature frequency was studied. The first frequency parameter is rapidly increased with the increase of small elastic coefficient (linear spring, $K_1 < 10$). However, it is slowly increased when $K_1 > 10$. Frequency parameters, especially first frequency parameter depend on parameter $K_1 (< 10)$ (linear spring) markedly and depend on parameter K_2 (screw spring) slowly. The influence of dimensions of the laminar diaphragm on the nature frequency was also studied. The frequency values decreased rapidly with the increase of the diaphragm diameter, especially in the small diameter range. The

first frequency of a diaphragm versus the thickness ratio of PZT layer to total layer of the plate was constructed for the purpose in the design of actuator or sensors in MEMS applications.

Acknowledgement

This research work is supported by National Natural Science Foundation of China (No. 10672111).

References

- [1] Shuichi W., Minoru S., Hiroshi G., Masashi T. and Tsuneji Y., "Static Characteristic of Piezoelectric thin Film Buckling Actuator," *Jpn. J. Appl. Phys.*, **35**, 5012-5014, (1996).
- [2] Lebedev M., Akedo J. and Akiyama Y., "Actuation Properties of Lead Zirconate Titanate thick Films Structured on Si Membrane by the Aerosol Deposition Method," *Jpn. J. Appl. Phys.*, **39**, 5600-5603, (2000).
- [3] Tsurumi T., Ozawa S., Abe G., Ohashi N., Wada S. and Yamane M., "Preparation of $\text{Pb}(\text{Zr}_{0.53}\text{Ti}_{0.47})\text{O}_3$ Thick Films by an Interfacial Polymerization Method on Silicon Substrates and their Electric and Piezoelectric Properties," *Jpn. J. Appl. Phys.*, **39**, 5604-5608, (2000).
- [4] Surowiak Z., Czekaj, D. Bakirov A. A. and Dudkevich V. P., "Dynamical Deformation Sensors based on thin Ferroelectric PZT Films," *Thin Solid Films*, **256**, 226-233, (1995).
- [5] Tang Y. Y. and Xu K., "Dynamic Analysis of a Piezothermoelastic Laminated Plate," *J. Thermal Stresses*, **18**, 87-104, (1995).
- [6] Batra R. C. and Liang X. Q., "The Vibration of a Rectangular Laminated Elastic Plate with Embedded Piezoelectric Sensors and Actuators," *Comput. Struct.*, **63**, 203-216, (1997).
- [7] Ding H. J. and Chen W. Q., "New State Space Formulations for Transversely Isotropic Piezoelectricity with Applications," *Mech. Res. Commun.*, **27**, 319-326, (2000).
- [8] Benjeddou A. and Deü J. F., "A Two-dimensional Closed-form Solution for the Free-vibrations Analysis of Piezoelectric Sandwich Plates," *International Journal of Solids and Structures*, **39**, 1463-1486, (2002).
- [9] Saravanos D. A., Heyliger P. and Hopkins D. A., "Layerwise Mechanics and Finite Element for the Dynamic Analysis of Piezoelectric Composite Plates," *Int. J. Solids Struct.*, **34**, 359-378, (1997).
- [10] Correia V. M. F., Gomes M. A. A., Suleman A., Soares C. M. M. and Soares C. A. M., "Modeling and Design of Adaptive Composite Structure," *Comput. Meth. Appl. Mech. Eng.*, **185**, 325-346, (2000).
- [11] Ha S. K. and Kim Y. H., "Analysis of a Piezoelectric Multimorph in Extensional and Flexural Motions," *Journal of Sound and Vibration*, **253**, 1001-1014, (2002).
- [12] Ha S. K., "Analysis of the Asymmetric Triple-layered Piezoelectric Bimorph using Equivalent Circuit Models," *Journal of the Acoustical Society of America*, **110**, 856-864, (2001).
- [13] Percin G. and BT K. Y., "Piezoelectrically Actuated Flexensional Micromachined Ultrasound Transducers - I: Theory," *IEEE Trans. Ultrason., Ferroelect., Freq. Contr.*, **49**, 573-584, (2002).
- [14] Percin G., "Plate Equations for Piezoelectrically Actuated Flexural Mode Ultrasound Transducers," *IEEE Trans. Ultrason., Ferroelect., Freq. Contr.*, **50**, 81-88, (2003).
- [15] Heyliger P. and Saravanos D. A., "Exact Free-vibration Analysis of Laminated Plates with Embedded Piezoelectric Layers," *J. Acoust. Soc. Am.*, **98**, 1547-1557, (1995).
- [16] Xu K. M., Noor A. K. and Tang Y. Y., "Three-dimensional Solutions for Free Vibrations of Initially-stressed Thermoelastoelectric Multilayered Plates," *Computer Methods in Applied Mechanics and Engineering*, **141**, 125-139, (1997).
- [17] Ricketts D., "The Frequency of Flexural Vibration of Completely free Composite Piezoelectric Polymer Plates," *J. Acoust. Soc. Amer.*, **80**, 723-726, (1986).
- [18] Yang J. S., Batra R. C. and Liang X. Q., "The Vibration of a Simply Supported Rectangular Elastic Plate due to Piezoelectric Actuators," *Int. J. Solids Struct.*, **33**, 1597-1618, (1996).
- [19] Chang S. H. and Tung Y. C., "Electro-elastic Characteristics of Asymmetric Rectangular Piezoelectric Laminae," *IEEE Trans. Ultrason., Ferroelect., Freq. Contr.*, **46**, 950-960, (1999).
- [20] Chaudhr Z., Lalande F. and Rogers C. A., "Modeling of Induced Strain Actuation of Shell Structure," *J. Acoust. Soc. Amer.*, **97**, 2872-2877, (1995).
- [21] Tzou H. S. and Gadre M., "Theoretical Analysis of a Multi-layered thin Shell Coupled with Piezoelectric Shell Actuators for Distributed Vibration Controls," *J. Sound Vib.*, **132**, 433-450, (1989).
- [22] Adelman N. T. and Stavsky Y., "Flexural-extension Behaviour of Composite Piezoelectric Circular Plates," *J. Acoust. Soc. Amer.*, **67**, 819-822, (1980).
- [23] Rudnitiskii S. I., Sharapov V. M. and Shul'ga N. A., "Vibration of a Bimorphic Disk Transducer of the Metal-piezoceramic Type," *Sov. Appl. Mech.*, **26**, 973-980, (1990).

- [24] Evseichik Y. B., Rudnitskii S. I., Sharapov V. M. and Shul'ga N. A., "Sensitivity of a Metal-piezoceramic Bimorph Transducer," *Sov. Appl. Mech.*, **26**, 1174-1181, (1990).
- [25] Yao L. Q., Lu L., Wang Z. H., *et al.*, "Exact Solution of Multi-layered Piezoelectric Diaphragm", *IEEE Trans. Ultrason., Ferroelect., Freq. Contr.*, **50**, 1262-1271, (2003).
- [26] Reddy J. N., *Mechanics of Laminated Composite Plate Theory and Analysis*, CRC Press, Florida, USA (1997).
- [27] Reddy J. N., *Theory and Analysis of Elastic Plates*, Taylor & Francis, Philadelphia PA (1999).